Journal of Materials Chemistry A

Accepted Manuscript

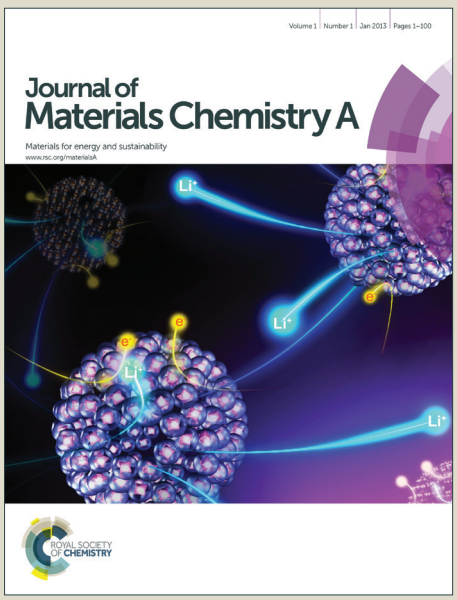

ROYAL SOCIETY OF CHEMISTRY

www.rsc.org/materialsA

Phonons, Lithium Diffusion and Thermodynamics of $LiMPO_4$ (M=Mn, Fe)

Prabhatasree Goel[a], M. K. Gupta[a], R. Mittal[a], S. Rols[b], S. J. Patwe[c], S. N. Achary[c], A. K. Tyagi[c] and S. L. Chaplot[a]

[1]*Solid State Physics Division, Bhabha Atomic Research Centre, Mumbai, 400085, India*

[2]*Institut Laue-Langevin, BP 156, 38042 Grenoble Cedex 9, France*

[3]*Chemistry Division, Bhabha Atomic Research Centre, Mumbai,400085, India*

We report phonon studies using neutron inelastic scattering experiments, ab-initio density functional theory calculations and potential model calculations on $LiMPO_4$ (M=Mn, Fe) at ambient and high temperature to understand the microscopic picture of Li sub-lattice. The experiments are in good agreement with calculations. Here for the first time we have correlated diffusion of lithium and dynamical instability in $LiMPO_4$. The lattice dynamics calculations indicate instability of zone-centre as well as zone-boundary phonon modes along [100] at unit cell volume corresponding to elevated temperature. At ambient condition, eigen vector of Li corresponding to these modes exhibit displacement only in the x-y plane. However with initiation of phonon instability Li atoms exhibit displacement along all the three directions with the highest component along x direction. Molecular dynamics simulations with increasing temperature indicate large mean square displacement of Li as compared to other constituent atoms. The computed pair-correlations between various atom pairs show that there is local disorder occurring in the lithium sub-lattice with increasing temperature, while other pairs show minimal changes.

Keywords: Neutron inelastic scattering, Phonon, *ab- initio* calculations, Lattice dynamics, Molecular dynamics simulation

PACS: 78.70.Nx, 63.20.-e, 63.20.Dj, 63.20.Dk

I. INTRODUCTION

Ever increasing energy demands has always promoted research for the elusive perfect battery material, thus paving way for a safer, secure, sustainable energy alternative[1-6]. Lithium transition metal phospho-olivines[7,8,9]have emerged as one of the leading contenders in this race. Since the time they were proposed by Padhi[7,8]et al, they have been actively considered as a potential and viable alternative to the conventional cathode materials like $LiCoO_2$. $LiMPO_4$ have large theoretical capacity[9,10] and a large operating voltage[4,9]. The importance is further accentuated by their stability[11,12], high safety, low cost, low toxicity and cyclability. The electrochemical[13-16]properties of these materials determine Li intercalation and deintercalation[15], vital to their functioning as useful electrode materials. They in turn are determined by their basic structural and thermodynamic properties. Despite enormous works pertaining to battery research,[13-19] many aspects of their basic vibrational and other physical properties have not been copiously studied. Studies on delithiated[20-24] $LiMPO_4$, solid solutions have been done to explore methods to increase conductivity in these compounds[20-28]. There have been several first principle studies of their electronic properties[28-33a], Li diffusion[34-39], easy direction of lithium diffusion[40-43], inelastic neutron scattering on unmixed and disordered $Li_{0.6}FePO_4$[44], magnetic behavior, theoretical studies on their vibrational properties and a few Raman, infrared studies on zone centre phonon modes[45-49].

At ambient conditions, these compounds crystallize in olivine type (Fig. 1) orthorhombic Pnma[50] space group analogous to mineral Triphylite structure. $LiMPO_4$ are paramagnets above their Neel temperatures. In case of $LiFePO_4$[51-53], below T_N= 50 K, Fe^{2+} spins align collinear with b-axis, while in $LiMnPO_4$[54,55] Mn^{2+} spins align along a-axis below T_N = 34 K. The structure comprises of discrete PO_4 tetrahdera and highly distorted oxygen octahedra about lithium and transition metal ion, M. The PO_4 tetrahdra are irregular, with two significantly different sets of O-O distances.

A rich collection of studies on these compounds relating to its technological applications are available in literature. But low electronic conductivity and low lithium diffusivity plague[56] the effective use of these compounds as battery materials. There have been several studies on methods[57-64] to overcome these limitations. There are reports on super-valence ion doping in Li-site, doping in M-site , nanocomposite LiFePO4/carbon powder, thermal treatment and carbon coating to improve upon its poor lithium transport in solid-state. There are studies to determine the preferable directions of Li diffusion, quantitative values of D_{Li} (diffusion coefficient)[24,65] in LiFePO4 using, muon spectroscopy[37,38] as well as first principles method. The chemical diffusion coefficient of Li has been studied using galvanostatic

intermittent titration technique[65-67]. Atomistic studies on the role of defects in Li transport have been studied[68]. Effect of non-stoichiometry, strain and doping on Li diffusion[69,70] in both LifePO4 and $LiMnPO_4$[24] has also been extensively studied. Carbon coating of $LiMPO_4$[58] and vacancies[40] in the lattice are found to increase the conductivity of these compounds. Previous electronic structure calculations[33(b)] found that $LiFePO_4$ compound shows half metallic behavior while $LiMnPO_4$ has insulating behaviour. The number of 3d electrons in $LiFePO_4$ and $LiMnPO_4$ are 6 and 5 respectively, leading to possible difference in bonding and volume.

Our interest in this study has been to understand the dynamics of these compounds and plausible role of phonons in triggering the lithium ion movement. In this paper we have studied phonons in the entire Brillouin zone, softening of phonons with increasing volume, diffusion of lithium and microscopic picture of the disturbances occurring in the lattice with increasing temperature. Here we report for the first time the inelastic neutron scattering measurements of the phonon density of states and its calculation using shell model as well as *ab-initio* approach. The model calculations are in good agreement with the inelastic neutron scattering data and *ab-initio* calculations. This allowed testing of our model, which is used to explore the possibility of Li diffusion using molecular dynamics simulations. Section II and III provide details on the inelastic neutron scattering investigations and the computations respectively. Section IV discusses the various results obtained along with their significance. The conclusions obtained from our work are given in Section V.

II. EXPERIMENTAL

Polycrystalline samples of $LiMnPO_4$ and $LiFePO_4$ were synthesized by the solid state reaction of appropriate reactants. $LiMnPO_4$ was synthesized from the stoichiometric ratio of $NH_4MnPO_4.H_2O$ and Li_2CO_3 in argon atmosphere at 750 °C. $NH_4MnPO_4.H_2O$ was prepared by precipitation from $MnCl_2$ solutions using aqueous ammonia. $LiFePO_4$ was synthesized by the reaction between Li_2CO_3, Fe_2O_3 and $NH_4H_2PO_4$ and glucose at 700 °C in flowing N_2 atmosphere. Glucose was used as reagent for reducing Fe^{3+} to Fe^{2+}.

The inelastic neutron scattering measurements of the phonon density of states in the polycrystalline samples of $LiMPO_4$ (M=Mn,Fe) has been performed using the IN4C time of flight spectrometer at the Institut Laue-Langevin (ILL), in Grenoble, France. About 10 grams of polycrystalline samples were used in thin aluminum foil. Sample thickness was about 2 mm. The measurements at 300 K were performed in the neutron-energy gain mode with incident neutron energy

of 14.2 meV (2.4 Å). The elastic energy resolution is 0.5 meV. The energy resolution of the instrument varies from a minimum of 0.5 meV to 10% of the energy transfer. The detector bank covered scattering angles from 10° to 110°. The signal is corrected for the contributions from the empty cell and suitably averaged over the angular range using the available software package at ILL. A standard vanadium sample was used to calibrate the detectors.

In the incoherent[71(a)] one-phonon approximation the measured scattering function $S(Q,E)$, as observed in the neutron experiments, is related to the neutron cross-section weighted phonon density of states as follows:

$$g^{(n)}(E) = A < \frac{e^{2W_k(Q)}}{Q^2} \frac{E}{n(E,T) + \frac{1}{2} \pm \frac{1}{2}} S(Q,E) > \qquad (1)$$

$$g^{n}(E) = B \sum_{k} \{ \frac{4\pi b_k^2}{m_k} \} g_k(E) \qquad (2)$$

where the + or – signs correspond to energy loss or gain of the neutrons, respectively, and $n(E,T) = \left[\exp(E/k_B T) - 1\right]^{-1}$. A and B are normalization constants and b_k, m_k, and $g_k(E)$ are, respectively, the neutron scattering length, mass, and partial density of states of the k^{th} atom in the unit cell. The quantity within < ---- > represents an appropriate average over all the neutron momentum transfer (Q) values at a given energy. $2W(Q)$ is the Debye-Waller factor, which was set to zero. The weighting factors $\frac{4\pi b_k^2}{m_k}$ for each atom type in the units of barns/amu are: Li: 0.196; Fe: 0.208 ; Mn: 0.039; P: 0.107 and O: 0.265 calculated from the neutron scattering lengths.[72]

III. COMPUTATIONAL DETAILS

The lattice dynamics calculations has been performed using both empirical potential[73-75] as well as *ab-initio* methods. Density functional theory (DFT) has been shown to describe the structural and lattice dynamical properties of material using pseudopotentials and plane wave basis sets. In the frame work of density functional perturbation theory (DFPT)[76] it is possible to calculate phonon frequencies, dielectric constants, and other properties. We have used the Vienna ab initio simulation package

(VASP-5.2) [77,78] along with the PHONON package for the phonon calculations. The volume dependence of zone centre and zone boundary phonon modes has been calculated using density functional perturbation theory implemented in VASP. The plane wave pseudo-potential has been used with maximum plane wave energy cutoff of 500 eV for these compounds. The integrations over the Brillouin zone has been performed on a 4×7×9 grid of k-points generated by Monkhorst[79,80] pack method. The generalized gradient approximation (GGA) exchange correlation given by Perdew Burke and Ernzerhof [79] with projected–augmented wave method has been used. $LiMPO_4$ (M=Fe, Mn) has 28 atoms in a unit cell. First-principles calculations have been carried out for the ground states of A-type AFM structures of $LiMPO_4$. The on-site Hubbard interaction for the d-electrons has been taken care within the approach as introduced by Dudarev[81] et al. The value of the onsite interaction term U=4.3 eVfor d electrons for Fe and Mn has been taken from previous studies[45(a)] on $LiMPO_4$ (M=Mn, Fe). For the phonon calculation, we have used a 1×2×2 super cell of the primitive unit cell. A total 112 atoms are contained in the super-cell. The convergence criteria for the total energy and ionic forces were set to 10^{-8} eV and 10^{-5} eV $Å^{-1}$, respectively. Total energies and inter-atomic forces were calculated for the 16 structures resulting from individual displacements of the three symmetry in equivalent atoms along the three Cartesian directions (±x, ±y and ±z). Phonon frequencies were extracted from subsequent calculations using the PHONON software.[82]

DFPT method can be used to calculate the phonon frequencies at any given specific q point, However in the force constant approach using the PHONON code one can obtain the phonons in the entire Brillouin zone, but it is very time expensive. DFPT method has been used to calculate the volume dependence of the zone-boundary and zone center modes specifically. These calculations have been used to identify the dynamically unstable regime. Later the force constant approach has been used for calculation of phonon spectra in the entire Brillouin zone at unit cell volumes corresponding to ambient as well as dynamically unstable regime. The results obtained from either method are identical except for the longitudinal optic modes that are not obtained in the DFPT method.

Our empirical calculations have been carried using interatomic potentials consisting of Coulomb and short-range Born-Mayer type interaction terms. The form of the interatomic potential used in our model is given by the following expression:

$$V(r) = \frac{e^2}{4\pi\varepsilon_0}\frac{Z(k)Z(k')}{r} + a\,\exp\left(\frac{-br}{R(k)+R(k')}\right) - \frac{C}{r^6}$$

Where, a=1822 eV and b=12.364 are empirical constants. We have successfully used this set of parameters in the lattice dynamical calculations of several complex solids. The term C_{ij} =100 eVÅ^6 accounts for the van der Waals interaction between O-O pairs. The effective charge Z(k) and radii R(k) parameters used in our calculations are Z(Li)= 1.0 , Z(Fe/Mn)= 1.869 Z(P)= -3.581.6, Z(O)= -1.6125 , R(Li)= 1. 35 Å, R(Fe)= 1.88 Å, R(Mn)= 1.91 Å , R(P)= 1.20,and R(O)= 1.65 Å. The polarizability of the oxygen atoms is introduced in the framework of the shell model[75]. The shell charge and shell core force constants for oxygen atoms are −2.00 and 60 eV/Å^2 respectively. The parameters of the potentials satisfy the conditions of static and dynamic equilibrium. The calculations have been carried out using the current version of DISPR.[83]

Classical molecular dynamics calculations have been carried out to understand the diffusion of lithium ions with increasing temperature. The interatomic potential parameters are the same as those obtained from our lattice dynamics simulations except that the oxygen polarizability was not included. The evolution of the super cell consisting of 7056 ions (4**a** × 7**b** × 9**c**) has been carried out in the NPT ensemble. The mean-square displacements of atoms and pair correlation between pairs of atoms have been calculated using the simulations.

IV. RESULTS AND DISCUSSION

A. Phonon Density of States

The measured neutron inelastic scattering spectra at room temperature with incident neutron energy of 14.2 meV are shown in Fig.2. The geometrical constraints of the instruments have allowed collecting the data from about 1 to 7 Å^{-1}. We find that for data summed over 1 to 7 Å^{-1} the phonon spectra of both the $LiMPO_4$ (M=Mn, Fe) consist of a strong peak between 0 and 8 meV. The Raman and infrared measurements do not indicate zone-centre optic modes at such low energies[45-47].In order to understand the origin of the peak, experimental data were grouped in two different regimes namely, high Q (4 to 7 Å^{-1}) and low Q (1 to 4 Å^{-1}) respectively. We find that for high Q data the intensity of the low energy excitations between 0 and 5 meV have decreased strongly, while low Q data indicate substantial increase in intensity of the same peak. The magnetic signal is expected[84] to be more pronounced at low Q, and decrease strongly at high Q, following the magnetic form factor.

Further S(Q,E) plots for $LiMPO_4$ (M=Mn, Fe) are shown in Fig. 3. As mentioned above both the compounds have antiferromagnetic ordering below 50 K. The Fe[51-53] and Mn[54,55] compounds show antiferromagnetic ordering below 52 K and 35 K respectively. Strong intensity at 300 K around 5 meV in $LiFePO_4$ is due to paramagnetic scattering of the compounds. In case of $LiMnPO_4$ paramagnetic scattering is below 3 meV. The magnetic scattering is seen (Fig. 3) as a broad quasi elastic like signal centered around 0 meV in the S(Q,E). When transforming this spectrum of relaxation origin into a density of state spectrum (Eq. (1)) this feature transforms into a peaked function. This peak is clearly seen (Fig. 2) in the $g^{(n)}(E)$ spectra of $LiFePO_4$ and $LiMnPO_4$ at around 5 meV and 3 meV respectively. There are already experimental data[52, 54] on the presence of magnetic excitations below the Neel temperatures, where energy of such excitations is around 5 meV in $LiFePO_4$; and below 3 meV in $LiMnPO_4$. Hence we can consider the lowest energy peaks in these compounds at 300 K to be due to paramagnetic scattering.

Fig. 4 gives the neutron weighted density of states of the powder samples in $LiFePO_4$ and $LiMnPO_4$ in comparison with the calculated model potential results and ab-initio calculations. The multiphonon spectra have been calculated using the Sjolander[71(b)] formalism and subtracted from the experimental data. The phonon spectrum extends up to 150 meV. The experimental spectrum consists of several peaks at 25, 55, 75 and 120 meV. No modes are observed for energies between 85 and 105 meV. The general characteristics of the experimental features are well reproduced by the calculations. The measurements are found to be in agreement with our model as well as *ab-initio* calculations. The parital contribution of the constituent atoms to the total phonon density of states in the two olivines computed using both model and *ab-initio* calculations is shown in Fig. 5. We find that Fe/Mn ions contribute largely below 40 meV, while Li being lighter contributes up to 75 meV. The density found beyond 105 meV is only due to the stretching modes of the PO_4 polyhedra. Further the comparison of calculated partial density of states (Fig. 5) of various atoms from both the approaches indicates difference in the phonon spectra for lithium atoms above 40 meV. The potential model parameters have been fitted to reproduce the experimental data as closely as possible apart from satisfying static and dynamic equilibrium, while there is no fitting involved in the ab-initio calculations. We can say that vibrations of the Li atoms have been better represented by the potential model in comparison with the ab-initio method.

B. Behavior of Phonons with Volume

The phonon dispersion has been calculated along the high symmetry directions using potential

model as well as *ab-initio* method. In general the calculated nature of dispersion relation is nearly same from both the methods, as also reflected in the calculated density of states (Figs. 4 and 5). Fig. 6 shows the calculations of phonon dispersion relations using the *ab-initio* method. The LO-TO (longitudinal optic and transverse optic) splitting of the modes has also been included while plotting the phonon dispersion relation. The phonon frequencies are usually expected to soften with increase of volume. Our previous studies on Li_2O[85,86] show that the zone-boundary transverse-acoustic phonon mode along [110] softens at volume corresponding to the superionic transition. The phonon frequencies of $LiMPO_4$ (M=Mn,Fe) have been calculated (Fig. 7) using *ab-initio* method as a function of volume. The phonon frequencies along all the three high symmetry direction are found to soften with increase of volume. However, the softening is found to be very large for one of the zone-centre (ZC) and zone- boundary (ZB) modes along [100] direction. The change in the phonon frequency with increasing volume (Fig. 8) has been plotted for these ZC and ZB modes. We find that in both the compounds the zone centre optic mode softens first, followed in quick succession by the zone-boundary mode with increasing volume. The thermal expansion behaviour as calculated from molecular dynamics calculations (as discussed below in Section IVB) indicates that $LiFePO_4$ exhibits phonon softening at computed unit cell volume corresponding to 1500 K while similar phenomena occurs at 900 K in $LiMnPO_4$. This region is hitherto defined by us as dynamically unstable regime. The detailed studies of the diffusion of Li in the two compounds are discussed in section IV D below.

For qualitative understanding of the atomic displacement in these unstable modes, we have plotted eigen vectors of both these modes (Fig. 9). In case of ZC mode at ambient volume the displacements of the Li atoms is maximum, while the amplitudes of other atoms are less but not negligible. The displacement of the lithium ions is only in the x-y plane. In the dynamically unstable regime, the amplitude of Li atoms has increased significantly. The Fe atoms are at rest, while the amplitude of P atoms decreased slightly and O atoms do not show any change. The component of displacement of Li atoms is non-zero along all the three directions but with the highest component along x direction.

For ZB mode (Fig. 9), all the atoms have finite displacement in the ambient regime. In case of lithium, there is no displacement along z-direction while the displacements along x and y directions are comparable. Here again movement is only in the x-y plane. While in the high temperature regime, the amplitude of Fe and P atoms have reduced substantially and there is a large increase in amplitude of Li atoms. It is interesting to note that Li atoms at the corners of the unit cell do not show any substantial change in amplitude. This behavior is different as compared to the ZC mode where amplitude of all Li

atoms increased simultaneously. As far as O atoms are concerned, the amplitudes do not change. Careful analysis of the eigen vector of ZB mode also indicates that, there are non-zero components along all the three directions. The component along z-direction is least, while the largest component is along x-direction.

From both the analysis we can see that at ambient temperature, the likely motion of lithium is in the x-y plane. If conducive conditions prevail, lithium might move in this plane. Earlier calculations and experimental observation[37-41] of thermal ellipsoids of lithium ions from neutron diffraction at ambient temperature have shown that lithium ions move along y-direction in a curved path. Hence as far as room temperature results are concerned our results are in agreement with previous observations. But, with substantial increase in temperature, we find that the scenario changes.

We find that $LiFePO_4$ shows softening (Fig. 8) at a higher volume in comparison with the Mn counterpart. The percentage change in volume for initiation of phonon instability in $LiMnPO_4$ is much lesser as compared to $LiFePO_4$. This may point to the fact that the onset of increased mean-squared amplitude (MSD) of lithium, in $LiMnPO_4$ might occur at a lower temperature. The phonon instabilities observed at higher volume may correspond to higher lithium MSD compared to the ambient volume. The main interest in these compounds stems from their use as battery materials. Lithium intercalation and subsequent delithiation are the main processes by which energy is transferred during its use as battery material. We have so far tried to unveil the role of phonons in the initiation of lithium movement crucial for the use of these materials as battery material.

C. Thermal Expansion, Diffusion Coefficient and Pair Correlation Function

Molecular dynamics simulations have been carried out using a supercell of 7056 atoms to study its evolution with increasing temperature. The system has been allowed to evolve for 80 picoseconds at each temperature. The thermal expansion of $LiMPO_4$ (M=Mn,Fe) has been calculated using model potentials in the quasiharmonic approximation and molecular dynamics simulations. The results have been compared with available experimental data[22,45a] in Fig. 10. There is a slight deviation between the calculated and experimental thermal expansion for $LiFePO_4$. The quasiharmonic calculations agree very well with the molecular dynamics simulations, suggesting that there are not very explicit temperature effects in the lattice with increasing temperature.

At 300 K, the galvanostatic and potentiostatic[65-67] intermittent titration of the most diffusing member has yielded values between 10^{-14} and 10^{-18} m^2/s for diffusion of lithium (D_{Li}) ions in solid solution of Li_xFePO_4 and $Li_{1-x}FePO_4$ ($X < 0.02$), respectively. GITT, electrochemical impedance spectroscopy (EIS) and cyclic voltammetry (CV) have been carried out to obtain D_{Li}[65,66,67]in thin films of $LiFePO_4$, these values are also in the order of 10^{-14} m^2/s. Self diffusion coefficient of Li^+ at 300 K measured using Mossbauer, muon-spin relaxation[37,38] is 3.6 x 10^{-14} m^2/s in $LiFePO_4$. Experimental visualization[40,41] of lithium diffusion has been reported in delithiated $Li_{0.6}FePO_4$. The diffusion of the constituent atoms in $LiMPO_4$ (M=Mn,Fe) was monitored in our molecular dynamics simulations. As expected lithium exhibits maximum mean square displacement as seen in Fig. 11 in both the compounds, which is very good agreement with Zhang et al[43] and Islam et al[68]. But we did not notice any perceivable diffusion (comparable to that of liquids, i.e of the order of 10^{-9} m^2/s) of lithium from our results, which indicates that diffusion coefficient is well below 10^{-10} m^2/s, beyond the scope of our molecular dynamics simulations. Yang *et al* have carried out ab-initio molecular dynamics study [42] to understand Li diffusion mechanism in $LiFePO_4$. The authors find that there is no macroscopic diffusion till 2000 K, beyond 2000 K Li diffuses in a curvaceous path, thermal vibration of trapped Li ions is quite anisotropic with a preferred direction towards face-shared tetrahedral Li sites. The authors also discuss about another possibility of Li ion migration involving the formation of Li-Fe antisite defect. It has been concluded that Li diffusion in $LiFePO_4$ is far more complex than suggested by previous researchers[34-39,40,41,43]. This concludes that these compounds in the pure form cannot be considered to belong to the family of superionic conductors[85,86]. The coefficient of diffusion of lithium in these compounds is reported to be around 10^{-12} m^2/s, about three orders lower than that of a liquid (10^{-9} m^2/s), which is the typical value for a superionic conductor. The various experimentally reported values of D_{Li} in the literature are found to be several orders of magnitude lesser than reported calculated values. The experimentally measured D_{Li} falls in the range of 10^{-17} to 10^{-11} m^2/s, which is the range suitable for a cathode material, hence finds extensive use in rechargeable batteries.

The pair correlations between two atoms indicate the probability of finding a given type of atom with respect to the atom considered. Fig. 12(a) and (b) show the pair correlation between various ion pairs in both the compounds at different temperatures. The correlation between Li ions shows some noticeable changes with increasing temperatures; at 1100 K there are some subtle changes in the atomic arrangement of lithium .This shows that with increase in temperature, there are readjustments occurring continuously in the Li-sub-lattice. In case of correlations between Fe-P, Li-P and Li-Fe there are very small changes indicating that the positions of these atoms have not changed with respect to each other. There are some small changes in the correlations between Fe-O, P-P, Li-O, Fe-Fe and O-O. The P-O

correlations are virtually undisturbed with increase in temperature, suggesting that PO_4 unit remains rigid, but there are some discernable changes in the orientations of the PO_4 polyhedra, particularly with respect to Li-sublattice. The correlations between Li-O show discernable changes at 1100 K as against the room temperature results. These results are in agreement with those of Zhang et al[43]. The behavior of the two olivines is similar with increase in temperature. Nevertheless the disturbance in the lattice appears to be very little and does not suggest large scale diffusion in case of both the compounds. The presence of well defined correlation peaks at higher temperature, of the various pair points out to the fact that the compounds are stable and increased disturbances in lithium sub-lattice is a local effect and does not bring about any drastic change to the overall lattice.

V. CONCLUSIONS

This work reports the study of the vibrational and thermodynamics properties of battery materials, $LiFePO_4$ and $LiMnPO_4$. A combination of inelastic neutron scattering, model lattice dynamics, molecular dynamics simulations and first principles calculations has been successfully used to understand the phonon dynamics and high temperature behavior in these compounds. The measured phonon density of states is in excellent agreement with our theoretical calculations. Our molecular dynamics simulations suggest that diffusion coefficient of lithium is less than 10^{-10} m^2/s in pure compounds, which is in agreement with reported results. Although lithium has maximum mean square displacement, it does not show any macroscopic diffusion, akin to a liquid. The pair correlation also suggest that there are subtle changes and disturbances occurring in the Li sub lattice, while PO_4 remains structurally unaffected even up to the highest temperatures studied. The phonon density of states calculated using first principles at volume corresponding to high temperature (> 1000 K) in $LiFePO_4$ and $LiMnPO_4$ suggests that there is a significant instability initiating in the Li sub-lattice. Analysis of the eigen vectors of these modes at 300 K suggest that if conducive conditions for Li movement from its lattice positions are available, the net displacement of Li atoms is in the x-y plane. But at higher temperature, the pattern of displacement suggests that lithium exhibits non-zero displacement along all the directions but with the highest component along x direction. Our calculations find the compounds to be thermally stable beyond 1000 K. Our exhaustive studies on their vibrational and thermodynamical properties will be useful in improving the utilization of $LiMPO_4$ (M=Mn,Fe) in numerous technological applications.

[1] J. M. Tarascon and M. Armand, Nature, 2001, **414**, 359.

[2] J. B Goodenough, Sol. Stat. Ionics,1994, **69**, 184.

[3] J. W. Fergus, J. Power Sources, 2010,**195,** 939.

[4] B. Scrosati and J. Garche, J. Power Sources, 2010,**195**, 2419.

[5] P. G. Bruce, Chem. Commun., 1997, **19**, 1817.

[6] M. S. Whittingham Chem. Rev., 2004, **104**, 4271.

[7] A. K.Padhi, K. S.Nanjundaswamy and J. B Goodenough., J. Electrochem. Soc., 1997, **144**, 1188

[8] A. K. Padhi, K. S. Nanjundaswamy, C. Masquelier, S. Okada and J. B. Goodenough, J. Electrochem. Soc., 1997, **144**, 1609 .

[9] Wu Borong, Ren Yonghuan and Li Ning, 2011. $LiFePO_4$ Cathode Material, Electric Vehicles" The Benefits and Barriers, Dr. Seref Soylu (Ed.), ISBN: 978-953-307-287-6, InTech, Available from: http://www.intechopen.com/books/electric-vehicles-the-benefits-and-barriers/lifepo4-cathode-material

[10] H. Huang, S. Yin and L. F. Nazar, Electrochem. Sol-St. Lett., 2001, **4**, A170; H. Matsuia, T. Nakamura, Y. Yamada, Y. Kobayashib, 15th international meeting on Lithium Batteries-IMLB 2010, electrochemical Society

[11] S. Anna Andersson,, John O. Thomas, Beata Kalska, and Lennart Häggström, Electrochem. and Solid-State Lett., 2000, **3,** 66; A. B. Mayza, M. Ramanathan, R. Radhakrishnan, S.Ha, V. Ramani., J. Prakash and K. Zaghib, ECS Trans., 2011, **35**, 177.

[12] P. S. Herle, B. Ellis, N. Coombs and L. F. Nazar, Nat. Mater., 2004, **3**, 148.

[13] Y. Xu, S. Chung, J. T Bloking., Y Chiang. and W. Y.Ching, Elect. Sol-St. Lett., 2004, **7**, A131.

[14] A. Yamada, Y. Kudo and K. Liu, J. Elect. Soc., 2001, **148**, A747.

[15] R. Malik, F. Zhou, G. Ceder, Nat. Mater., 2011, **10**, 587; C, Delmas,.; M. Maccario,.; L Croguennec,.; F. L Cras,.; F.Weill, Nat. Mater., 2008, **7**, 665; W. C. Chueh, F. E. Gabaly, J. D. Sugar, N. C. Barlelt, A. H. McDaniel, K. R. Fenton, K. R. Zavadil, T. Tyliszczak, W. Lai and K. F. Mccarty, Nano Lett., 2013, **13**, 866.

[16] B. Ellis, L. K. Perry, D. H. Ryan and L. F. Nazar, J. Am. Chem. Soc., 2006, **128**, 11416.

[17] R. Amin, J. Maier, P. Balaya, D. P. Chen and C. T. Lin, Sol. St. Ion., 2008, **179**, 1683.

[18] M.S. Whittingham, Y. Song, S. Lutta, P. Y. Zaalij, N. A. Chernova, J. Mat. Chem.,2005 **15**, 3362

[19] S. Chung, J. T. Bloking and Y. Chiang, Nat. Mater., 2002, **1**, 123.

[20] A. Yamada, H. Koizumi, S. Nishimura, N. Sonoyama, R. Kanno, M Yonemura, T. Nakamura and Y. Kobayahi, Nat. Mater., 2006, **5**, 357.

[21] A. S. Andersson and J. O Thomas, J. Power Sources, 2001, **97-98,** 498 .

[22] S. Kim, J. Kim, Gwon Hyeokjo and K. Kang, J. Electro. Society, 2009, **156,** A635.

[23] C. Delacourt , P. Poizot, J. Tarascon and C. Masquelier, Nat. Mat., 2005, **4**, 254.

[24] D. Morgan, Van der Van and G. Ceder, Electrom. Solid-State Lett., 2004, **7**, A30.

[25] F. Zhou, C. A. Marianetti, M. Cococcioni, D. Morgan and G. Ceder, Phys. Rev. B, 2004 **69**, 201101 (R).

[26] S Shi, L. Liu, C. Ouyang, D. Wang, Z. Wang, L. Chen and X. Hunag Phys. Rev. B, 2003, **68**, 195108.

[27] A. Yamada, Y. Kudo and K. Liu, J. Electrochem. Soc., 2001, **148,** A1153.

[28] F. Zhou, T. Maxisch and G. Ceder, Phys. Rev. Lett., 2006, **97**, 155704.

[29] M. K. Kinyanjui, P. Axmann, M Wohlfahrt-Mehrens, P. Moreau, F. Boucher and U. Kaiser, J. Phys: Condens. Matter, 2010, **22**, 275501.

[30] L. Wang, F. Zhou, Y. S. Meng and G. Ceder, Phys Rev. B, 2007, **76**, 165435.

[31] P. Tang and N. A. W. Hozwarth, Phys. Rev. B, 2003, **68**, 165107.

[32] S. Shi, C. Ouyang, Z. Xiong, L. Liu, Z. Wang, H. Li, D. Wang, L. Chen and Z. Huang, Phys. Rev. B, 2005, **71**, 144404.

[33] (a) S. P. Ong, V. L. Chevrier and G. Ceder , Phys. Rev. B, 2011, **83**, 075112; (b)Y. Xu,W. Y. Ching and Y. M. Chiang, J. Appl. Phys., 2004, **95**, 6583.

[34] C. Ouyang, S. Shi, Z. Wang, X. Huang and L. Chen, Phys. Rev. B, 2004, **69**, 104303

[35] T. Maxisch, F. Zhou and G. Ceder, Phys. Rev. B, 2006, **73**, 104301 .

[36] Y. Asari, Y. Suwa and T. Hamada, Phys. Rev. B, 2011, **84**, 134113.

[37] J. Sugiyama, H. Nozaki, M. Harada, K. Kamazawa, Y. Ikedo, Y. Miyake, O. Ofer, M. Mansson, E. J. Ansaldo, K. H. Chow, G. Kobayashi and R. Kanno, Phys. Rev. B, 2012, **85**, 054111.

[38] J. Sugiyama, H. Nozaki, M. Harada, K. Kamazawa, O. Ofer, M. Mansson, J. H. Brewer, E. J. Ansaldo, K. H. Chow, Y. Ikedo, Y. Miyake, K. Ohishi, I. Watanabe, G. Kobayashi, R. Kanno, Phys. Rev. B, 2011, **84**, 054430.

[39] P. J. Baker, I. Franke, F. L Pratt., T.Lancaster, D.Prabhakaran, W Hayes and S. J. Blundell, Phys. Rev. B, 2011, **84** 174403.

[40] S. Nishimura, G.Kobayashi, K.Ohoyama, R.Kanno, M.Yashima and A.Yamada, Nat. Mater., 2008, **7,** 707.

[41] G.K.P. Dathar, D. Sheppard, K. J. Stevenson and G. Henkelman, Chem. Mater., 2011, **23**, 4032

[42] J. Yang and J. S. Tse, J. Phys. Chem. A, 2011, **115**, 13045 .

[43] P. Zhang, Y. Wu, D. Zhang, Q. Xu, J. Liu, X. Ren, Z. Luo, M. Wang and w. Hong, J. Phys. Chem. A, 2008, **112**, 5406.

[44] R. Stevens,, J. L. Dodd, M. G. Kresch, R. Yazami, and B. Fultz B. Ellis and L. F. Nazar J. Phys. Chem. B 2006**, 110***,* 22732.

[45] (a) S. L. Shang, Y.Wang, Z. G.Mei, X. D.Hui and Z. K.Liu, Journal of Mater. Chem., 2012, **22**, 1142; (b) S Shi, H.Zhang, X. M. Ke, C.Ouyang, M.Lei and Li. Chen, Phy. Lett. A, 2009, **373,** 4096.

[46] W.Paraguassu, P. T. C.Freire, V. Lemos, S. M.Lala, L. A.Montoro and J. M.Rosolen, J. Raman Spectrosc., 2005, **36,** 213.

[47] K. P. Korona, J.Paperska, M.Kaminska, A.Witowski, M.Michalska and L.Lipinska, Mat. Chem. and Phys., 2011, **127,** 391.

[48] T Maxisch and G.Ceder, Phys. Rev. B, **2006, 73**, 174112.

[49] A. Hunt, W. Y. Ching, Y. M. Chiang and A. Moewes, Phys. Rev. B, 2006, **73**, 205120

[50] S.Geller and J. L.Durand, Acta Cryst., 1960, **13,** 325

[51] R. P. Santaro and R. E. Newnham, Acta Cryst., 1967, **22**, 344

[52] J. Li, V. O. Garlea, J. L. Zarestky and D. Vaknin, Phys. Rev. B, 2006, **73**, 024410

[53] G. Liang, K. Park, J. Li, R. E. Benson, D. Vaknin, J. T. Markert and M. C. Croft, Phys. Rev. B, 2008, **77**, 064414

[54] J. Li, W. Tian, Y. Chen, J. L. Zarestky, J. W. Lynn and D. Vaknin, Phys. Rev. B, 2009, **79**, 144410

[55] D. Aron, A. Zorko, R. Dominko and Z. Jaglicic, J. Phys: Condens. Matt.,2004, **16**, 5531

[56] C. Wang and J. Hong, Electrochem. Solid-State lett., 2007, **10,** A65

[57] B. Wu, Y. Ren, D. Mu, C. Zhang, X. Liu and F. Wu, Int. J. Electrochem. Sci., 2013, **8**, 8502

[58] M. M. Doeff, Y. Hu, F. McLarnon and R. Kosteckib, electrochemical and Solid-state Lett;, 2003, **10**, A207

[59] B. Delacourt, P. Poizot, S. Levasseur and C. Masqueliera, Electrochemical and Solid-State Letters, 2006, **9**, A352

[60] C. K. Park, S. B. Park, H. C. Shin, W. I. Cho and H. Jang, Bull. Korean Chem. Soc., 2011, **32**, 191

[61] J. M. tarascon, C. Delacourt, A. S. Prakash, M. Morcrette, M. S. Hegde, C. Wurm and C. Masquelier, Dalton Trans., 2004, P2988

[62]J. Lee, S. J. Pennycook and S. T. Pantelides., Appld. Phys. Lett., 2012, **101**, 033901

[63]H. Shao, Solid State Commun. 2010, **150**, 81

[64]C. R. Sides, F. Croce, V. Y. Young, C. R. Martin and B. Scrosatic, Elec. Solid-St. Lett., 2005, 8, A484

[65] A. V. Churikov, A. V. Ivnishchev, I. A. Ivanishcheva, V. O. Sycheva, N. R. Khasanova, E. V. Antipov, Electrochim. Acta, 2010, **55**, 2939.

[66] K.Tang, X.Yu, J.Sun, H.Li, X.Huang, Electrochim. Acta, 2011,**56,** 4869.

[67] P. P. Posini, M. Lisi, D. Zane, M. Pasquali, Solid-State. Ion., 2002, **148**, 45

[68] M. S.Islam, D. J.Driscoll, C. A. J. fisher and P. R.Slater, Chem Mater., 2005, **17**, 5085.

[69] S.Chung, S.Choi, T.Yamamoto and Y. Ikuhara, Phy. Rev. Lett., 2008, **100**, 125502.

[70] S.Chung, S. Choi, S. Lee and Y.Ikuhara, Phys. Rev. Lett., 2012,**108**, 195501.

[71] (a) D. L. Price and K. Skold, in *Methods of experimental physics: Neutron scattering Part A*, edited by K. Skold and D. L. Price (Academic Press, Orlando, 1986), Vol. **23**; J. M. Carpenter and D. L. Price, Phys. Rev. Lett., 1985, **54**, 441. (b) A. Sjolander, Arkiv fur Fysik, 1958, **14**, 315.

[72]www.ncnr.nist.gov; V. F. Sears, Neutron News, 1992, **3**, 29; A. -J. Dianoux and G. Lander (Eds.), Neutron Data Booklet, Institut Laue-Langevin, Grenoble, France.

[73] S. L. Chaplot, N. Choudhury, S. Ghose, M. N. Rao, R. Mittal and K. N. Prabhatasree, European Journal of Mineralogy,2002, **14**, 291.

[74] R. Mittal, S. L. Chaplot and N. Choudhury, Progress of Materials Science,2006, **51**, 211.

[75] G. Venkatraman, L. Feldkamp and V. C. Sahni, Dynamics of Perfect Crystals (MIT, Cambridge).

[76] S. Baroni, P. Giannozzi, and A. Testa, Phys. Rev. Lett., 1987, **58**, 1861.

[77] G. Kresse and J. Furthmüller, Comput. Mater. Sci., 1996, **6**, 15.

[78] G. Kresse and D. Joubert, Phys. Rev. B, 1999, **59**, 1758 .

[79] H. J. Monkhorst and J. D. Pack, Phys. Rev. B, 1976, **13**, 5188

[80] J. P. Perdew, K. Burke, and M. Ernzerhof, Phys. Rev. Lett., 1996, **77**, 3865

[81] S. L. Dudarev, G. A. Botton, S. Y. Savrasov, C. J. Humphreys and A. P. Sutton, Phys. Rev. B, 1998, **57**, 1505

[82] K. Parlinksi, Software phonon, 2003.

[83] S. L. Chaplot, Unpublished.

[84] G.E Bacon, *Neutron diffraction*, Oxford University Press, Oxford (1975).

[85] M. K. Gupta, P. Goel, R. Mittal, N. Choudhury and S. L. Chaplot, Physical Review, 2012, B **85**, 184304.

[86] P. Goel, N. Choudhury and S. L. Chaplot, J. Nucl Mater., 2008, **377**, 438

Fig.1 Structure of $LiMPO_4$ (M=Mn, Fe) (orthorhombic Pnma space group) derived from *xcrysden* software at T = 0 K. Key; Li: Red spheres, M=Mn or Fe: Yellow spheres, P: Green spheres, O: Blue spheres.

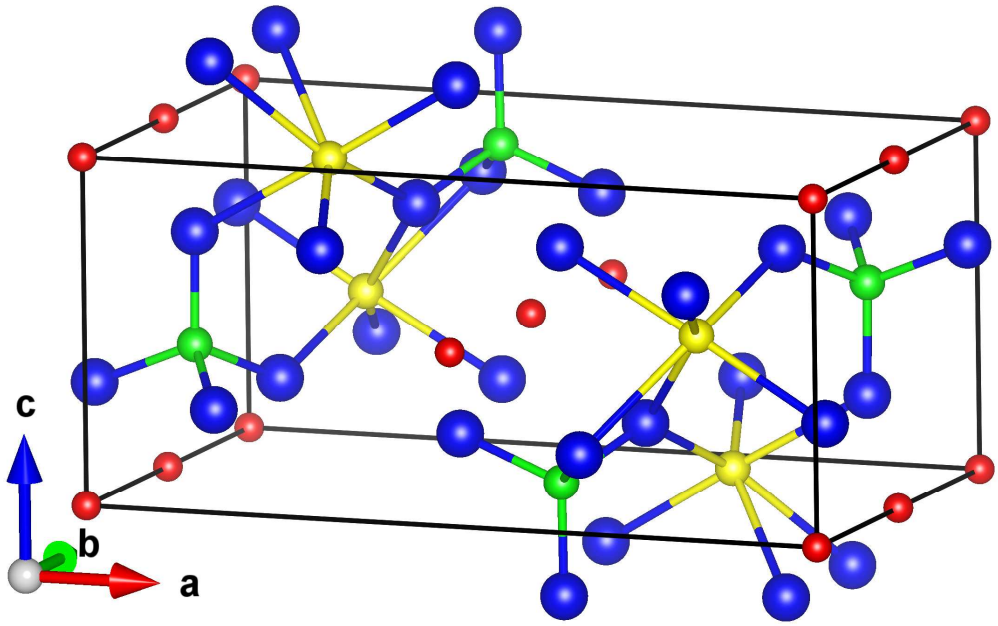

Fig. 2 The experimental neutron inelastic scattering spectra of $LiMPO_4$ (M=Mn, Fe) at 300 K. For better visibility the low Q and high Q spectra are shifted along the y-axis by 0.005 meV^{-1} and 0.01 meV^{-1} respectively.

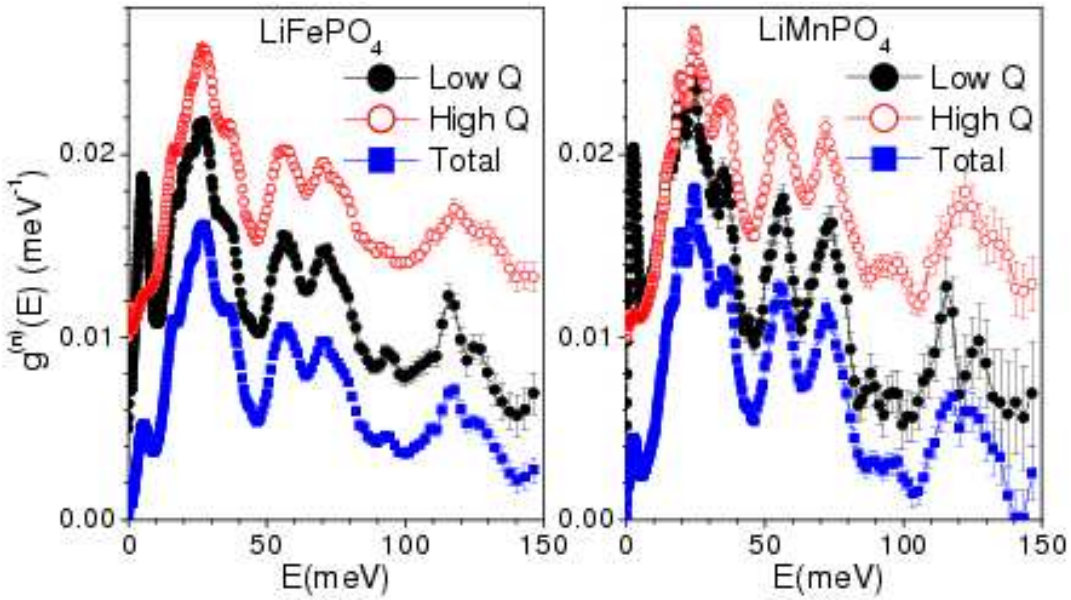

Fig. 3 The experimental S(Q,E) plots for $LiMPO_4$ (M=Mn, Fe) at 300 K.

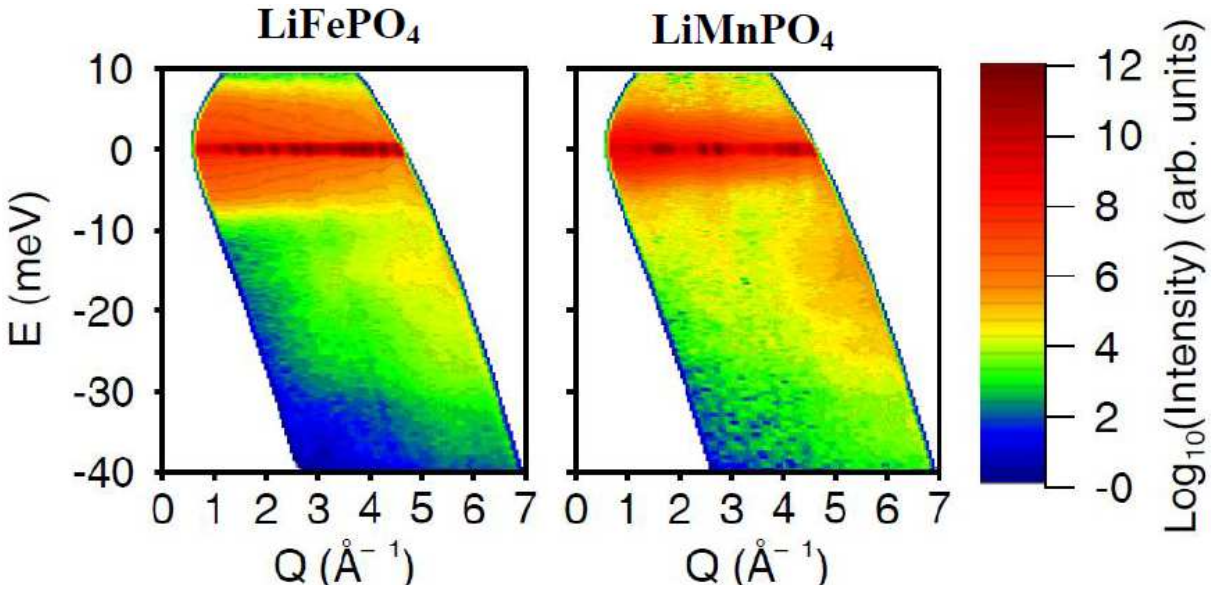

Fig. 4 The comparison of the calculated and experimental neutron inelastic scattering spectra for $LiMPO_4$ (M=Mn, Fe) at ambient pressure at 300 K. The *ab-initio* as well as potential model calculations are carried out at 0 K. The multi-phonon contribution calculated using the Sjolander formalism[71(b)] has been subtracted from the experimental data. The experimental spectra comprises of magnetic and phonon contribution, while computed results pertain to phonon contribution alone.The calculated spectra have been convoluted with a Gaussian of FWHM of 0.5 meV to 10% of the energy transfer in order to describe the effect of energy resolution in the experiment.

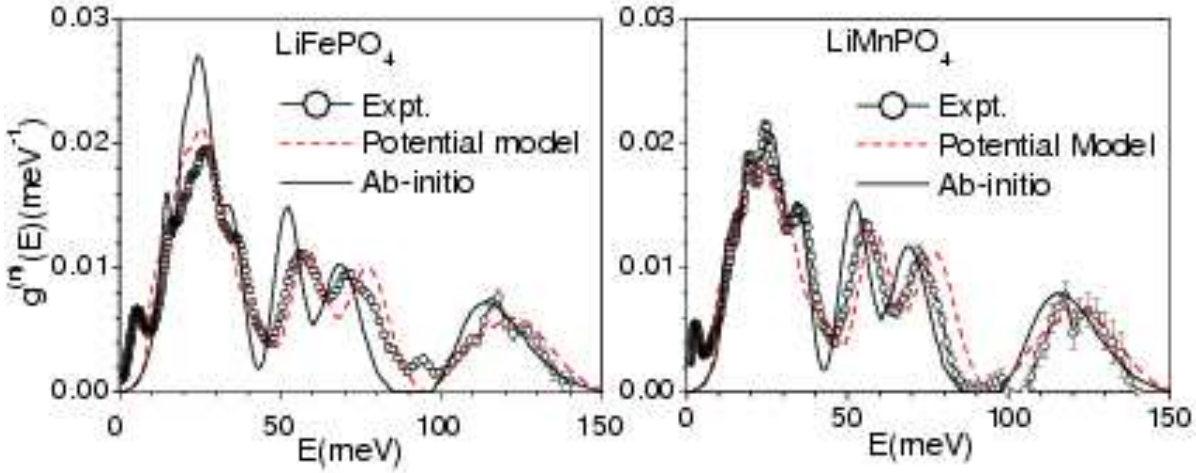

Fig. 5 The calculated partial densities of states in $LiMPO_4$ (M=Mn,Fe). The solid and dashed lines correspond to the calculations carried out using *ab-initio* and potential model.

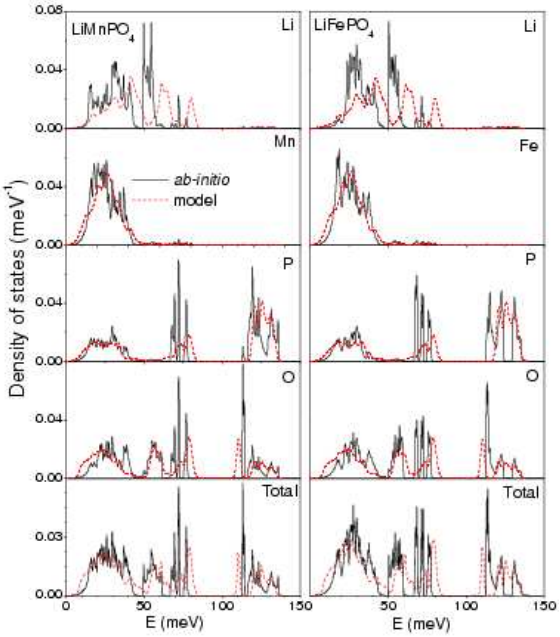

Fig. 6 The Calculated phonon dispersion for $LiMPO_4$ (M=Mn, Fe) from *ab-initio* density functional theory under generalized gradient approximation (GGA-DFT).

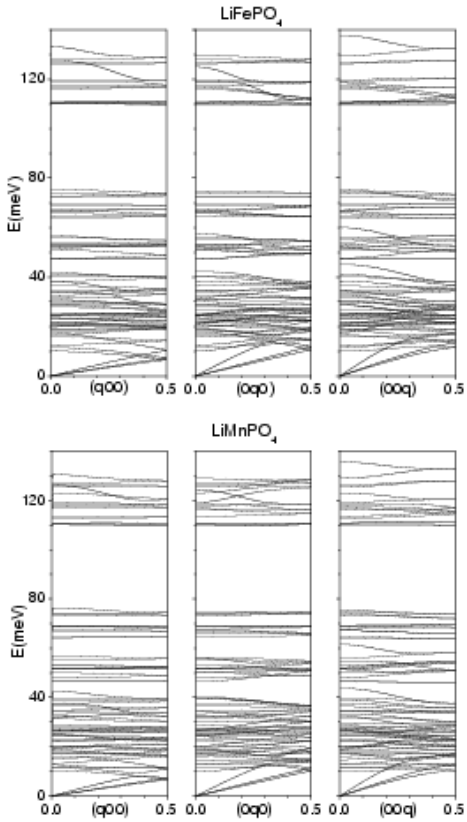

Fig. 7 The low-energy part of the phonon dispersion relation from *ab-initio* density functional theory under generalized gradient approximation (GGA-DFT). The full and dashed lines refer to the phonon dispersion corresponding to calculated unit cell parameters a=10.42(10.55) Å, b = 6.06 (6.17) Å, c = 4.75 (4.79) Å and a = 10.77 (10.66) Å, b = 6.20 (6.22) Å, c = 4.88 (4.83) Å for $LiFePO_4$ ($LiMnPO_4$). The zone-centre and zone-boundary phonon modes in $LiFePO_4$ and $LiMnPO_4$ soften at unit cell volume corresponding to the higher temperature. This region is hitherto defined by us as dynamically unstable regime. The thick lines shows the phonon branches undergoing large softening in the dynamically unstable regime.

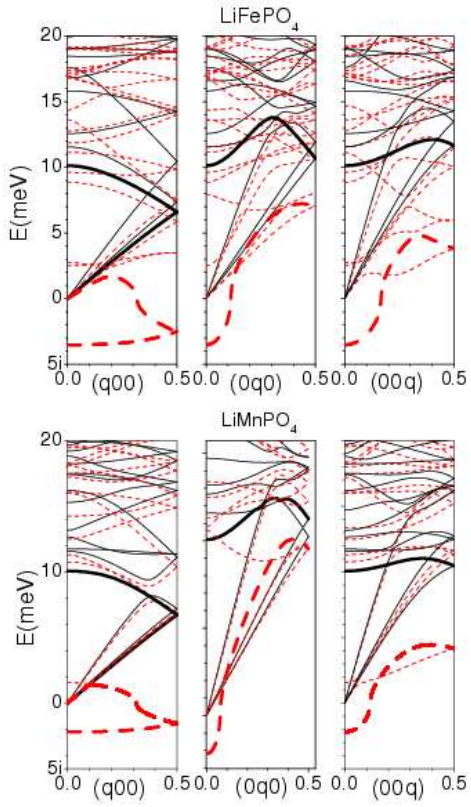

Fig. 8 Zone-boundary and zone-centre modes as a function of unit cell volume. The zone-centre and zone-boundary phonon modes in $LiFePO_4$ and $LiMnPO_4$ soften at unit cell volume corresponding to higher temperatures.

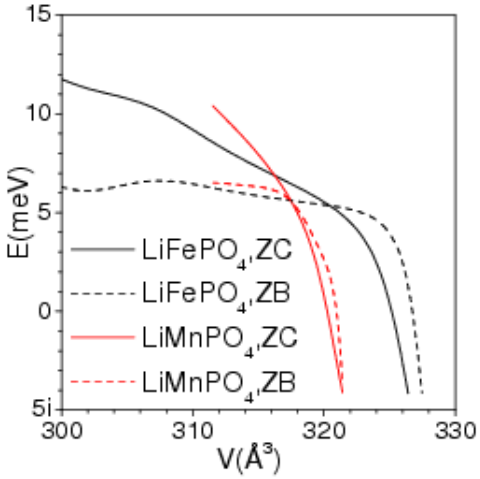

Fig. 9 Motion of individual atoms for zone boundary and zone centre modes at unit cell volumes corresponding to ambient and dynamically unstable region. The numbers after the mode assignments give the phonon energies of mode in Fe(Mn) compound. *i* after the phonon energy indicates that mode is unstable. A 2×1×1 super cell of the primitive unit cell is shown for zone boundary mode at (0.5 0 0). The lengths of arrows are related to the displacements of the atoms. The zone-centre and zone-boundary phonon modes in $LiFePO_4$ and $LiMnPO_4$ soften at unit cell volume corresponding to higher temperatures. The absence of an arrow on an atom indicates that the atom is at rest. Key; Li: Red spheres, M=Mn or Fe: Yellow spheres, P: Green spheres, O: Blue spheres.

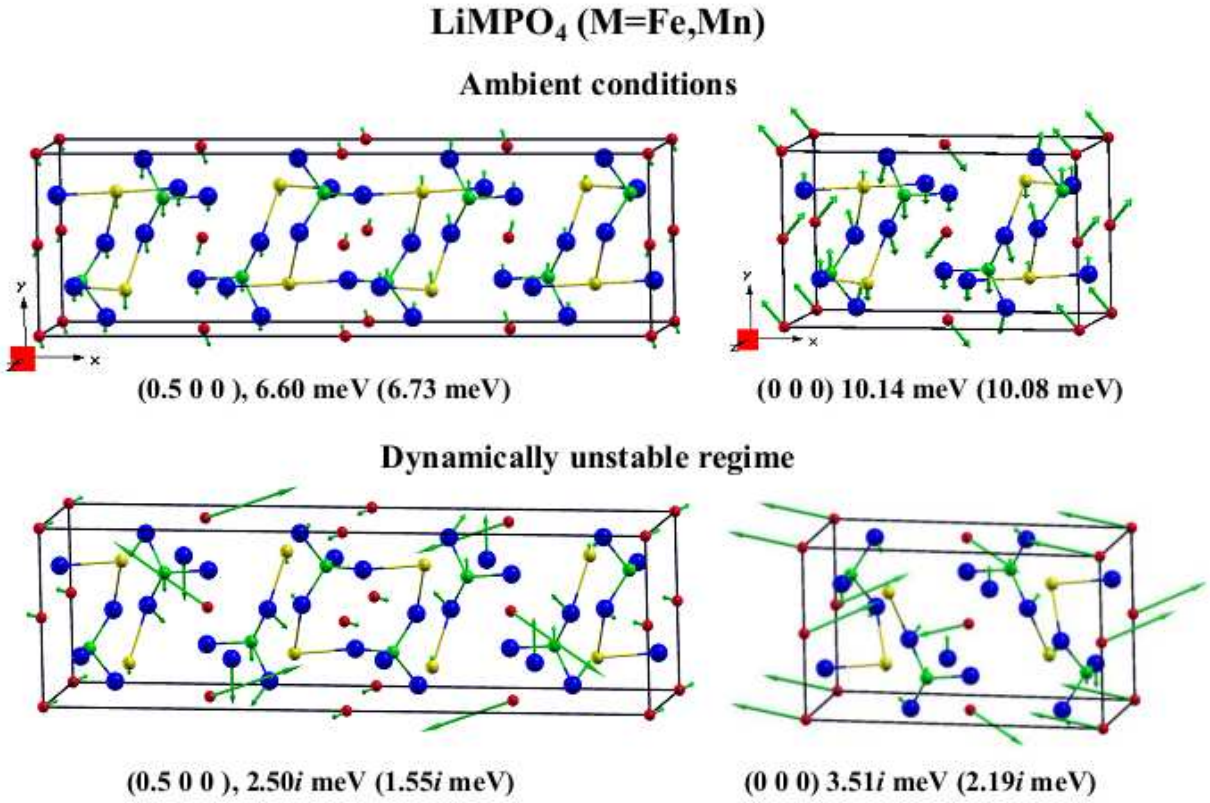

Fig. 10 Comparison between the experimental[22,45(a)] and calculated volume thermal expansion of $LiMPO_4$ (M=Mn, Fe). The dashed and full lines correspond to classical lattice dynamics (LD) and molecular dynamics (MD) calculations respectively.

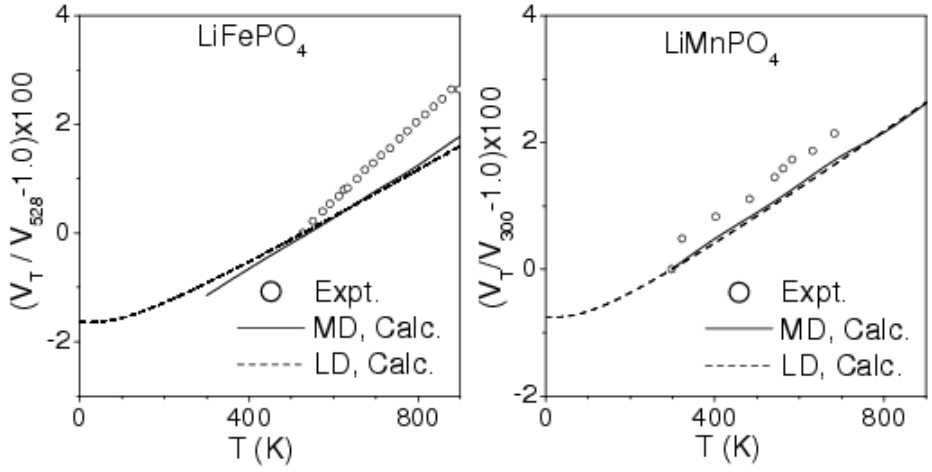

Fig.11 Mean-Squared Displacement of constituent atoms in $LiFePO_4$ and $LiMnPO_4$ with increasing temperature using molecular dynamics simulations.

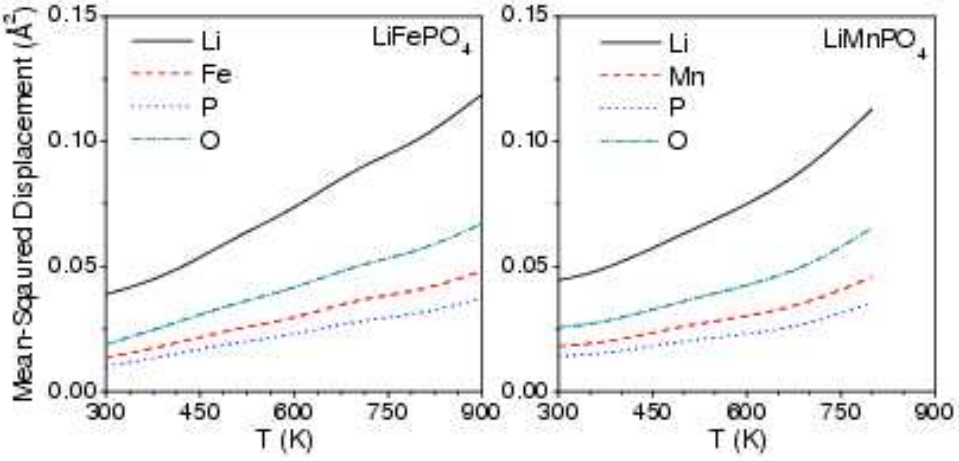

Fig. 12 Pair correlation function of different pairs of atoms in the olivines at various temperatures; 300K - Solid line ; 1100 K- dashed line.